Hindawi
International Journal of Antennas and Propagation
Volume 2023, Article ID 6666997, 6 pages
https://doi.org/10.1155/2023/6666997

Research Article

A High-Efficient Method for Synthesizing Multiple Antenna Array Radiation Patterns Simultaneously Based on Convolutional Neural Network

Shiyuan Zhang, Chuan Shi, and Ming Bai

The School of Electronic Information Engineering, Beihang University, Beijing, China

Correspondence should be addressed to Ming Bai; mbai@buaa.edu.cn

Received 19 July 2023; Revised 18 September 2023; Accepted 20 September 2023; Published 17 October 2023

Academic Editor: Arpan Desai

This paper proposes a high-efficient method that utilizes deep learning technology for synthesizing multiple antenna array radiation patterns simultaneously. More in details, the mathematical feasibility of using neural networks to optimize and synthesize radiation patterns of antenna arrays is demonstrated. Boundary functions are designed to reshape the important characteristics of target radiation patterns and transform them into a two-channel mask matrix, allowing for the simultaneous input of multiple target radiation patterns into the neural network without sacrificing computational efficiency. During training, the cost function is designed to represent the difference between each synthesized radiation pattern and the corresponding target radiation pattern, guiding self-learning. The main framework of the method is a convolutional neural network, where the convolutional layer is used to reduce the expansion of input parameters due to the simultaneous input of multiple mask matrices. Simulation experiments have been conducted to synthesize multiple incoherent target radiation patterns simultaneously on a patch antenna array layout, and the computation time is compared with the combined time required to compute each one individually. The results demonstrate that this method offers the advantage of computational efficiency for simultaneous synthesis of multiple incoherent radiation patterns.

1. Introduction

Antenna arrays are an effective means for radar and communication electronic systems to obtain antenna beams with strong directionality, low sidelobe, and easy scanning and beamforming capabilities [1–4]. The radiation pattern of an antenna array with excellent performance can be obtained by solving the excitations of each antenna element. Based on this, many radiation pattern synthesis methods are proposed and developed, including mathematical optimization synthesis methods [5–7], global optimization algorithms [8–10], and convex optimization algorithms [11–13]. The rapid development of deep learning technology [14–16] has drawn the attention of numerous antenna researchers, resulting in the creation of several neural network frameworks aimed at addressing challenges in the field of antenna [1, 17]. When it comes to radiation pattern synthesis, a variety of neural network methods have been proposed and developed [18–20], which can be broadly classified into two main types. The first category is the numerous training samples driven method. The neural network is pretrained on a large dataset to learn the relationship between the target radiation patterns and the element excitations. As a result, the trained neural network gains the ability to generalize and solve problems related to radiation pattern synthesis. The second category is the optimal approximation method for radiation patterns. In this method, the neural network constantly adjusts its own parameters during training to ultimately approximate the mapping between the target radiation patterns and the element excitations.

For synthesizing multiple radiation patterns, almost all optimization methods and synthesis techniques require each pattern to be synthesized individually, and the computational efficiency and results will be affected by the initial

evolutionary sample. Inspired by the fact that neural networks can effectively approximate almost any mapping, a high-efficient method based on convolutional neural networks is proposed for synthesizing multiple antenna array radiation patterns simultaneously. The universal approximation theorem of nonlinear input-output mapping is utilized to demonstrate the mathematical feasibility and establish a link between deep learning networks and solving the problem of radiation pattern synthesis, which is rare in similar research. Moreover, a multiparameter control expression is proposed to restrict the radiation characteristics of the target radiation pattern, so that multiple targets can be input simultaneously without compromising the computational efficiency. Through simulation experiments, we have successfully synthesized multiple incoherent radiation patterns on a patch antenna array layout and compared the calculation time with the combination time required to calculate each one individually.

2. Feasibility Proof of Solving Radiation Pattern Synthesis by Neural Network

Assuming that an antenna array consisting of n radiation elements is arranged in the XOY plane, the far-field pattern $\mathrm{FF}(\theta, \varphi)$ in any direction (θ, φ) is as follows:

$$\begin{aligned} \mathrm{FF}(\theta,\varphi) &= w^H A(\theta,\varphi), w = \left[w_1, w_2 \cdots, w_n\right]^T, \\ A(\theta,\varphi) &= \left[a_1(\theta,\varphi)\mathrm{AF}_1, \cdots, a_n(\theta,\varphi)\mathrm{AF}_n\right]^T, \\ \mathrm{AF}_i &= e^{-j\beta\left(x_i \sin\theta\cos\varphi + y_i \sin\theta\sin\varphi\right)}, \end{aligned} \tag{1}$$

where the excitation weight vector is denoted as w and $a_i(\theta, \varphi)$ represents the element pattern of the i-th antenna. The array factor $\mathrm{AF}_i(\theta, \varphi)$ is determined by the free-space wave number β and the position (x_i, y_i) in the coordinate system.

If the array factor and element pattern of each antenna are predefined, varying the excitation weight vector w can generate different far-field patterns $\mathrm{FF}(\theta, \varphi)$. Therefore, the problem of synthesizing the antenna array radiation pattern can be rewritten as finding the excitation weight vector w that maps to the target radiation pattern $\mathrm{FF}(\theta, \varphi)$, which can be achieved through the inverse function $w = F^{-1}(\mathrm{FF}(\theta, \varphi))$. It is evident that there exists a general mapping between the excitation weight vector w and the desired radiation pattern $\mathrm{FF}(\theta, \varphi)$. Interestingly, a trainable neural network structure can be used as a tool to implement this general mapping [21]. Hence, a neural network method is proposed to solve the inverse problem mentioned above. According to the universal approximation theorem of nonlinear input-output mapping, let $\sigma(\bullet)$ be a nonconstant, bounded, and monotone-increasing continuous functions. Let I_{m0} denote the $m0$-dimensional unit hypercube $[0, 1]^{m0}$. The space of continuous functions on I_{m0} is denoted by $\mathrm{C}(I_{m0})$. Then, given any function $f \ni \mathrm{C}(I_{m0})$ and $\varepsilon > 0$, there exists an integer $m1$ and sets of real constants a_k, b_k, and ω_{kq}, where $k = 1, \ldots, m1$ and $q = 1, \ldots, m0$ such that we may define the following:

$$F(s_1, \ldots, s_{m0}) = \sum_{k=1}^{m1} a_k \sigma\left(\sum_{q=1}^{m0} \omega_{kq} s_q + b_k\right), \tag{2}$$

as an approximate realization of the function $f(\bullet)$; that is,

$$\left|F(s_1, \ldots, s_{m0}) - f(s_1, \ldots, s_{m0})\right| < \varepsilon, \tag{3}$$

for all that lies in the input space $s_1, \ldots, s_{m0}$.

The linear calculation process in (3) is analogous to the forward superposition calculation principle used for synthesizing radiation patterns. Universal approximation theorem is directly applicable to neural network [21]. In the neural network, we note $\sigma(\bullet)$ as activation function and note that (3) represents the output of a neural network as follows: (1) the network has $m0$ input nodes and a single hidden layer consisting of $m1$ neurons; the inputs are denoted by $s_1, \ldots, s_{m0}$; (2) hidden neuron k has synaptic weights $\omega_{\mathrm{k1}}, \ldots, \omega_{\mathrm{m0}}$ and bias b_k; and (3) the network output is a linear combination of the outputs of the hidden neurons, with $a_1, \ldots, a_{\mathrm{m1}}$ defining the synaptic weights of the output layer.

The depth of the neural network can be enhanced by increasing the number of hidden layers, and (2) can be expressed in the following form of nested activation functions:

$$F(s, \omega, b) = \sigma\left(\sum_k \omega_{ok} \sigma\left(\sum_j \omega_{kj} \sigma\left(\cdots \sigma\left(\sum_l \omega_{lj} s_i + b_l\right)\right) + b_j\right) + b_k\right). \tag{4}$$

In this paper, the target pattern $\mathrm{FF}(\theta, \varphi)$ is treated as the function $f(\bullet)$ and the excitation weight vector w is taken as the output of the neural network. Then, by substituting (4) with (1), the output radiation pattern $\mathrm{FF_R}(\theta, \varphi)$ of the neural network during training is obtained:

$$\mathrm{FF_R}(\theta, \varphi) = F^H(s, \omega, b)\mathrm{A}(\theta, \varphi). \tag{5}$$

Based on the universal approximation theorem and (3), the radiation pattern $\mathrm{FF_R}(\theta, \varphi)$ output by the neural network after training will be the approximate realization of the target radiation pattern $\mathrm{FF}(\theta, \varphi)$.

3. Design of the Neural Network

3.1. Design of the Neural Network Input and Cost Function. In the target radiation patterns, the main beam direction, sidelobe level, and main beam width are typically the most crucial radiation characteristics. Therefore, it is not necessary to restrict all scanning angles, but only the scanning

angle region where the radiation properties of interest are present to limit. In this paper, we express the target radiation pattern $\mathrm{FF}(\theta, \varphi)$ as a function $f(\theta_1, \varphi_1, \theta_2, \varphi_2, \ldots, \theta_d, \varphi_g)$ and relax it to a space bounded by the upper boundary $\mathrm{UB}(\theta, \varphi)$ and lower boundary $\mathrm{LB}(\theta, \varphi)$. The upper boundary $\mathrm{UB}(\theta, \varphi)$ confines the desirable upper radiation features, such as the sidelobe level SLL and -3 dB width of the main beam $2\theta_w$, while the lower boundary $\mathrm{LB}(\theta, \varphi)$ limits the desirable lower radiation features, including the main beam direction (θ_0, φ_0) and, if necessary, the lowest level value V, which are defined by various parameters. To facilitate parallel data processing and improve computational efficiency, the two boundaries are transformed into a two-channel mask matrix with θ and φ as coordinate axes, as shown in Figure 1. Under these conditions, the neural network's output radiation pattern $\mathrm{FF_R}(\theta, \varphi)$ will satisfy

$$\mathrm{LB}(\theta, \varphi) \le \mathrm{FF_R}(\theta, \varphi) \le \mathrm{UB}(\theta, \varphi). \tag{6}$$

If there are S desired radiation patterns that need to be synthesized simultaneously, the s-th cost function $\mathrm{l}_s(w)$ is computed as the difference between the radiation pattern $\mathrm{FF}^s_{\mathrm{R}}(\theta, \varphi)$ and its corresponding mask matrix:

$$\begin{aligned} \mathrm{l}_s &= \nu_1^s \cdot \mathrm{Uloss}^s + \nu_2^s \cdot \mathrm{Vloss}^s, \\ \mathrm{Uloss}^s &= \frac{1}{D \cdot G} \left\| \max\left(0, \mathrm{FF}^s_{\mathrm{R}}\left(\theta_i, \varphi_j\right) - \mathrm{UB}^s\left(\theta_i, \varphi_j\right)\right) \right\|_2^2, \\ \mathrm{Vloss}^s &= \frac{1}{D \cdot G} \left\| \min\left(0, \mathrm{FF}^s_{\mathrm{R}}\left(\theta_i, \varphi_j\right) - \mathrm{LB}^s\left(\theta_i, \varphi_j\right)\right) \right\|_2^2, \end{aligned} \tag{7}$$

where D and G are the total number of sampling directions in the angular space (θ, φ). Different attention weight coefficients ν_1 and ν_2 are assigned to Uloss and Vloss for effective self-learning.

The pooling layer provides spatial and translational invariance to convolutions, allowing features to be detected regardless of their location in the input. However, for radiation pattern synthesis, the main beam direction is the critical information that the neural network must learn. As such, the output must be sensitive to the main beam direction information, which is described in the input. Thus, pooling layers must be removed between convolutional layers. After multiple convolutional layers, the critical information of the input is extracted and output. Finally, a few dense layers are constructed to integrate the global information output of the convolutional structure and map them to the sampling space. The detailed structure of the neural network is presented in Figure 1.

The number of convolution layers and dense layers can be chosen based on the following factors:

(1) The characteristics of the antenna array are the number of array elements, array spacing, and so on. For complex antenna arrays, more convolution layers may be necessary to extract additional information, and more dense layers may be required for information mapping.

(2) Design objectives of the radiation pattern: For the design objectives with high accuracy, such as the beam direction and peak radiation intensity of the antenna array, more convolution layers may be necessary to extract more precise information.

(3) Computing resources: The number of convolutional and dense layers must also consider the limitations of available computing resources. More convolutional layers and dense layers may require more computing resources, such as GPUs and longer training times.

In conclusion, the selection of the number of convolutional and dense layers should be based on the specific antenna design problem. Multiple experiments and adjustments may be required to determine the optimal number of convolutional and dense layers and other hyperparameters.

In this work, the structural parameters of the convolutional layer and dense layer are based on those of the AlexNet neural network, but all pooling layers are removed. The number of neurons in the output layer is related to the number of antenna units. Additionally, a batch normalization layer is added after each convolutional layer to enhance learning. To accelerate convergence and prevent gradient vanishing, the activation functions of all layers are set to "relu" except for the output layer which uses the "sigmoid" activation function to control the excitation weight vector w range.

It is noteworthy that in the training process, the function of backpropagation technique is to reduce the difference between the output radiation pattern $\mathrm{FF_R}(\theta, \varphi)$ and the target radiation pattern $\mathrm{FF}(\theta, \varphi)$. During the calculation, the output includes the amplitude and phase excitations of all antenna elements in the s-th group ($s = \{1, \ldots, S\}$), as shown in Figure 1. Forward propagation entails computing all the cost function l_s. The neural network continuously updates the network's parameters by identifying the direction of gradient reduction of all S-cost functions. Ultimately, all S synthesized radiation patterns meet their respective predefined requirements. For the backpropagation process, we used the "Adam" optimization algorithm to update the parameters of the neural network and seamlessly integrate it into the TensorFlow framework.

4. Numerical Examples

In this section, we demonstrate the successful simultaneous synthesis of five radiation patterns, each with a different main beam direction, using our proposed neural network framework. The numerical examples were implemented by the TensorFlow framework, which is supported by GPU-based acceleration, resulting in efficient and effective computation.

In the example, the radiation patterns are synthesized in the upper half space of the array for directions (θ, φ) and the layout of the antenna array is shown in Figure 2. The constructed mask matrices have a resolution of 1° for both θ and φ and have resolution 1° in the upper half space, resulting in $D = 360$ and $G = 90$. To optimize all radiation patterns, weight coefficients $\nu_1 = 1$ and $\nu_2 = 500$ are applied with a learning rate of $\mu = 5 * 10^{-6}$.

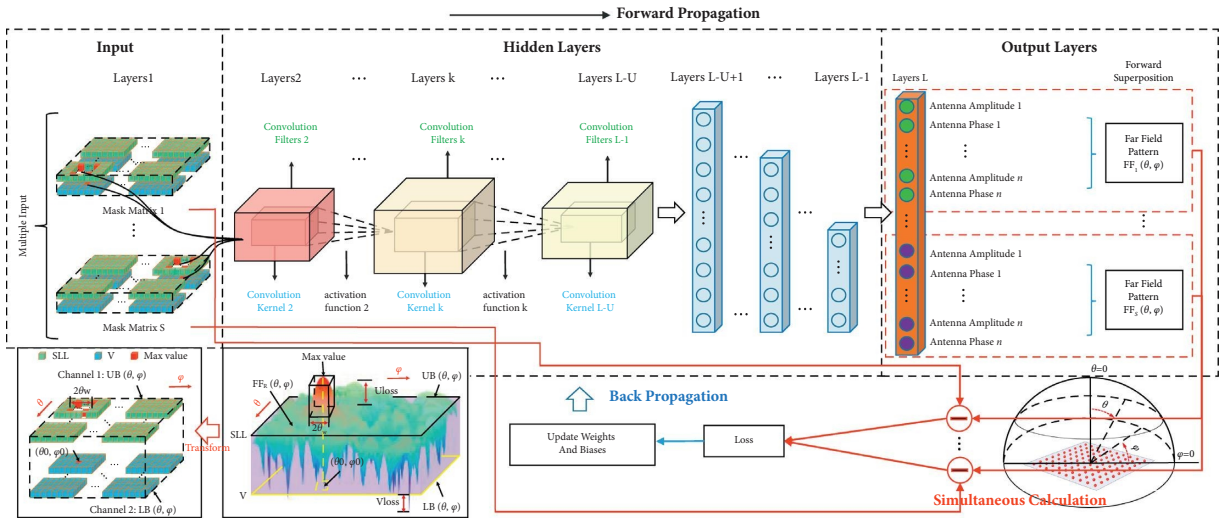

Figure 1: Structure diagram of the neural network and transformation of the mask matrix.

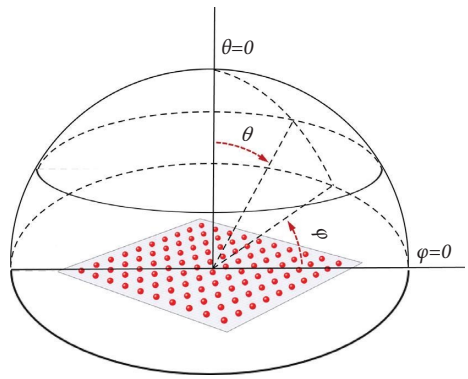

Figure 2: The layout diagram of antenna array elements (in the Ka band 28 GHz, a 100-element uniformly distributed patch antenna array is deployed in the *XOY* plane, with each antenna element spaced at half a wavelength).

The requirements for the five target radiation patterns outlined in this paper are as follows: each main beam direction needs to be pointed precisely in a different direction, and lower sidelobe levels can be achieved by setting the sidelobe level value to SLL = −18. The amplitude (normalized) and phase results of the radiation pattern with different main beam directions are shown in Figures 3 and 4, respectively, and the main radiation properties of the different results are shown in Table 1.

All the aforementioned results were synthesized simultaneously, taking only 87 seconds, which is a half of the combined time required to compute each one individually (185 seconds). This demonstrates the high efficiency of the proposed neural network framework in synthesizing multiple incoherent radiation patterns simultaneously.

5. Discussion

We believe that the reason behind this high efficiency is the unique computational approach in neural networks: First of all, backpropagation technology is one of the reasons to ensure the high efficiency of neural networks. And another point is that we add the convolutional layer structure as an important improvement over our previous work. The utilization of weight sharing and local connections in the convolutional layers serves to significantly reduce network parameters. This, in turn, allows for the deepening of the network while preserving computational efficiency. Furthermore, for synthesizing multiple antenna array radiation patterns simultaneously, adding the convolutional layer structure can also reduce the expansion of input parameters due to the simultaneous input of multiple mask matrices and further ensure computational efficiency. It is also worth noting that the appropriate selection of the learning rate, determined through several experiments, not only accelerates the learning efficiency but also leads to satisfactory results. Moreover, in the target radiation pattern presented in this paper, the direction of the main beams is the most important radiation characteristic, and thus the weight ν_2 associated with controlling the direction of the main beam is given a higher value. By increasing the weight ν_1 of the Uloss, which is related to controlling the sidelobe level, the sidelobe

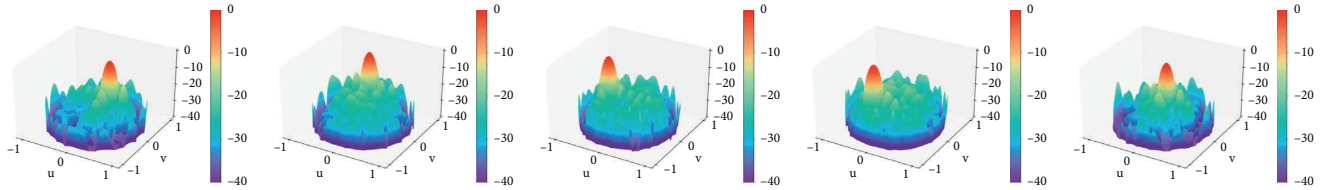

(a) (b) (c) (d) (e)

Figure 3: The amplitude results of the normalized radiation patterns.

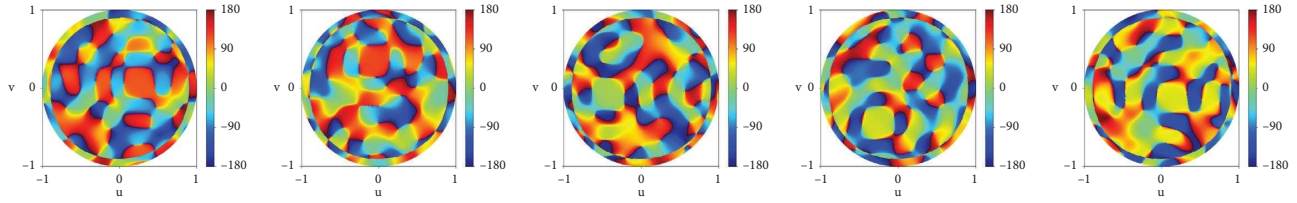

(a) (b) (c) (d) (e)

Figure 4: The phase results of the radiation patterns.

Table 1: Main radiation properties of the results.

Radiation properties	a	b	c	d	e
Main beam direction	15°, 15°	100°, 20°	190°, 25°	240°, 30°	320°, 10°
Sidelobe level (dB)	−12.6	−13.3	−14.2	−13.4	−12.6
Beam width (azimuth)	10°	10°	10°	10°	10°

level value in the result can be further reduced. The proposed neural network framework has the flexibility to synthesize more than five incoherent radiation patterns. However, increasing the number of radiation patterns synthesized will result in a larger input and output for the neural network framework. The ability of a neural network to process data concurrently is related to the number of neurons at each layer, and thus the number of neurons in each layer will also increase with the number of radiation patterns synthesized simultaneously. Furthermore, if this method is used for a larger antenna array, the number of neurons in the output layer must match the number of antenna units. Under the above circumstances, there is a greater demand for computing equipment and sufficient computing resources.

6. Conclusions

In this paper, we present a method for synthesizing multiple antenna array radiation patterns simultaneously, using CNN. Numerical examples demonstrate that the proposed method is highly efficient. Multiple parameters control the upper and lower boundary functions, allowing flexibility to reshape the various requirements of the target radiation patterns. Additionally, the transformation of the mask matrix not only facilitates parallel computation but also offers a method for the neural network to handle multi-objective optimization problems. The authors believe that utilizing the proposed neural network to simultaneously synthesize a large number of radiation patterns will offer higher computational efficiency advantages and can be extended to address many other electromagnetic field problems.

Data Availability

The data, models, or code used to support the findings of this study are available from the corresponding author upon request.

Conflicts of Interest

The authors declare that they have no conflicts of interest.

Acknowledgments

This work was supported by the Microwave Engineering Laboratory, Beihang University.

References

[1] Z.-J. Guo, Z.-C. Hao, H.-Y. Yin, D.-M. Sun, and G. Q. Luo, "Planar shared-aperture array antenna with a high isolation for millimeter-wave low earth orbit satellite communication system," *IEEE Transactions on Antennas and Propagation*, vol. 69, no. 11, pp. 7582–7592, 2021.

[2] M. Faenzi, D. Gonzalez-Ovejero, G. Petraglia et al., "A metasurface radar monopulse antenna," *IEEE Transactions on Antennas and Propagation*, vol. 70, no. 4, pp. 2571–2579, 2022.

[3] P. Mallick, M. Ameen, R. Chowdhury, A. K. Ray, and R. K. Chaudhary, "Wideband circularly polarized cavity-backed dielectric resonator antenna with low RCS for aerial vehicle communications," *IEEE Antennas and Wireless Propagation Letters*, vol. 21, no. 7, pp. 1418–1422, 2022.

[4] Y. Ye, X. Zhao, and J. Wang, "Compact high-isolated MIMO antenna module with chip capacitive decoupler for 5G mobile terminals," *IEEE Antennas and Wireless Propagation Letters*, vol. 21, no. 5, pp. 928–932, 2022.

[5] S. K. Goudos, G. S. Miaris, K. Siakavara, and J. N. Sahalos, "On the orthogonal nonuniform synthesis from a set of uniform linear arrays," *IEEE Antennas and Wireless Propagation Letters*, vol. 6, pp. 313–315, 2007.

[6] G. Freitas de Abreu and R. Kohno, "A modified Dolph-Chebyshev approach for the synthesis of low sidelobe beampatterns with adjustable beamwidth," *IEEE Transactions on Antennas and Propagation*, vol. 51, no. 10, pp. 3014–3017, 2003.

[7] S. Lei, H. Hu, B. Chen, P. Tang, J. Tian, and X. Qiu, "An array position refinement algorithm for pencil beam pattern synthesis with high-order taylor expansion," *IEEE Antennas and Wireless Propagation Letters*, vol. 18, no. 9, pp. 1766–1770, 2019.

[8] Q. Guo, Y. Wang, D. Yuan, J. Li, and T. Yu, "Optimization of sparse concentric ring arrays based on multiple constraints," *IEEE Antennas and Wireless Propagation Letters*, vol. 19, no. 5, pp. 781–785, 2020.

[9] Q. Xu, S. Zeng, F. Zhao, R. Jiao, and C. Li, "On formulating and designing antenna arrays by evolutionary algorithms," *IEEE Transactions on Antennas and Propagation*, vol. 69, no. 2, pp. 1118–1129, 2021.

[10] J. Yang, P. Yang, F. Yang, Z. Xing, X. Ma, and S. Yang, "A hybrid approach for the synthesis of nonuniformly-spaced linear subarrays," *IEEE Transactions on Antennas and Propagation*, vol. 69, no. 1, pp. 195–205, 2021.

[11] Q. Lu, G. Cui, R. Liu, and X. Yu, "Beampattern synthesis via first-order iterative convex approximation," *IEEE Antennas and Wireless Propagation Letters*, vol. 20, no. 8, pp. 1493–1497, 2021.

[12] Y. Gong, S. Xiao, and B. Wang, "Synthesis of nonuniformly spaced arrays with frequency-invariant shaped patterns by sequential convex optimization," *IEEE Antennas and Wireless Propagation Letters*, vol. 19, no. 7, pp. 1093–1097, 2020.

[13] Y. Li, Y. Gong, and S. Xiao, "Synthesis of modular subarrayed phased-array with shaped-beams by means of sequential convex optimization," *IEEE Antennas and Wireless Propagation Letters*, 2022.

[14] C. Du, C. Du, L. Huang, H. Wang, and H. He, "Structured neural decoding with multitask transfer learning of deep neural network representations," *IEEE Transactions on Neural Networks and Learning Systems*, vol. 33, no. 2, pp. 600–614, 2022.

[15] D. Kollias and S. Zafeiriou, "Exploiting multi-CNN features in CNN-rnn based dimensional emotion recognition on the OMG in-the-Wild dataset," *IEEE Transactions on Affective Computing*, vol. 12, no. 3, pp. 595–606, 2021.

[16] P. Zhang, J. Xue, C. Lan, W. Zeng, Z. Gao, and N. Zheng, "EleAtt-RNN: adding attentiveness to neurons in recurrent neural networks," *IEEE Transactions on Image Processing*, vol. 29, pp. 1061–1073, 2020.

[17] V.-P. Kutinlahti, A. Lehtovuori, and V. Viikari, "Optimizing RF efficiency of a vector-modulator-driven antenna array," *IEEE Antennas and Wireless Propagation Letters*, vol. 19, no. 12, pp. 2507–2511, 2020.

[18] J. P. Jacobs, "Accurate modeling by convolutional neural-network regression of resonant frequencies of dual-band pixelated microstrip antenna," *IEEE Antennas and Wireless Propagation Letters*, vol. 20, no. 12, pp. 2417–2421, 2021.

[19] T. Iye, P. V. Wyk, T. Matsumoto, Y. Susukida, S. Takaya, and Y. Fujii, "Neural network-based phase estimation for antenna array using radiation power pattern," *IEEE Antennas and Wireless Propagation Letters*, 2022.

[20] S. Zhang, D. Huang, B. Niu, and M. Bai, "High-efficient optimisation method of antenna array radiation pattern synthesis based on multi-layer perceptron network," *IET Microwaves, Antennas & Propagation*, vol. 16, no. 12, pp. 763–770, 2022.

[21] S. Haykin, "Neural networks and learning machines," vol. 3, Pearson, Upper Saddle River, NJ, USA, 2009.